Discussions

The deflection and bending moment at the center for the skew plate with aspect ratio equal to 1.0, 1.25, 1.5, and 2.0 and for included angles 75°, 60°, 45°, 30°, and 15° are calculated. The convergence of deflections and bending moments have been studied, by taking 3 and 5 terms. They are compared with available results. It should be noted that Iyengar and Srinivas obtained the values with 50 term series.

Deflections are given in Table 1. The values given by Kennedy are less than those here; and for large skew angles the difference is large. The values agree satisfactorily with those given by Iyengar and Srinivas.

Maximum principle bending moment coefficients at the center are compared with Iyengar's values in the graph (Fig. 2), Poisson's ratio is $\frac{1}{3}$.

As may be observed from the Table 1 that, the effect of increasing skew angle is to reduce the deflection and the effect of skew on maximum deflection decreases with the increasing aspect ratio.

References

[1] Mirsky, I., "The Deflection of a Thin Flat Parallelogram Plate under Pressure," ARL Rept. SM 175, 1951, Dept. of Supply, Australia.

[2] Otta, T. and Hamada, N., "Statistical Deflection of a Rhomboidal Plate with Clamped Edges Subjected to Uniformly Distributed Pressure," *Bulletin of Japan Society of Mechanical Engineers*, Vol. 6, No. 21, 1963, pp. 1–7.

[3] Warren, W. E., "Bending of Rhombic Plates," *AIAA Journal*, Vol. 2, No. 1, Jan. 1964, pp. 166–168.

[4] Morley, L. S. D., "Solution for Bending of a Clamped Rectangular Plate under Uniform Normal Load," *Quarterly Journal of Mechanics and Applied Mathematics*, Vol. 16, 1963, pp. 109–114.

[5] Kennedy, J. B., "On Bending of a Clamped Skew Plate under Uniform Pressure," *Journal of the Royal Aeronautical Society*, Vol. 69, 1965, pp. 352–355.

[6] Iyengar, K. T. S. R. and Srinivas, R. S., "Clamped Skew Pkates under Uniform Normal Loading," *Journal of the Royal Aeronautical Society*, Vol. 71, 1967, pp. 139–140.

[7] Gaydon, F. A. and Shephard, W. M., "Generalized Plane Stress in a Semi-Infinite Strip under Arbitrary 'End Load'," *Proceedings of the Royal Society of London*, Vol. 281, 1964, pp. 184–206.

Position Determination from Star-Gravity Measurements

R. H. KIDD* AND J. N. DASHIELL†
TRW Systems Group, Houston, Texas
AND
T. J. BLUCKER‡
NASA Manned Spacecraft Center, Houston, Texas

Introduction

THIS paper presents a description of a computational technique to determine the position of an observer on the surface of a planet from measurements of the unit gravity direction and star line of sight directions. The uncertainty in the direction of the gravitational potential of the planet is shown to determine the limiting accuracy of the estimator. Numerical results are presented to illustrate the convergence properties of the filter and to compare the filter solutions for the successful Apollo landing missions with other solutions for the landing sites.

For the Apollo missions, the selenographic position coordinates for the Lunar Module have been determined by a variety of methods. Most of these solutions are obtained relative to the position of the orbiting Command Module. Experience has shown that orbital position uncertainties, rather than the errors in the measurement devices, limit the accuracy of these LM position solutions.

The methods to determine Lunar Module (or landmark) position, which are functions of the orbiter position, are a) Command Module optical line of sight tracking, b) Lunar Module rendezvous radar tracking (angles, range and range rate) of the Command Module from the lunar surface, c) lunar mapping (photography from Apollo and Lunar Orbiter missions) confirmed by crew visual observations, and, d) the latitude, longitude and radius of a position vector near the time of Lunar Module powered descent initiation is used with the measured incremental change from these three quantities down to the surface. The increments are determined by the primary Lunar Module guidance system, by the auxiliary guidance system, and by a ground based high-speed computer recursive filter.

The object of this paper is to present a filter technique for position determination, which is independent of an orbitor's position uncertainties, that processes measured star line of sight directions and measured gravity directions. A weighted least-squares filter is formulated and its accuracy is shown to be limited by the uncertainties of the gravitational potential model. The convergence properties of this filter are shown to be excellent.

The position solutions from this star-gravity method for three Apollo missions are presented and compared to the best estimates of the actual landing site locations. These comparisons show that the solution accuracy of this filter is comparable to the methods discussed previously.

Filter Development

The use of star vector and gravity vector measurements to determine position can be illustrated by considering the deterministic problem when only two measurements are available. These measurements are shown in Fig. 1, where $\mathbf{r}^T = [\cos\phi\cos\lambda, \cos\phi\sin\lambda, \sin\phi]$ is the position vector, ϕ is latitude, λ is longitude, α_i is the angle between the position vector and the ith star vector, and the superscript T denotes the transpose operation.

If the measurements are the cosine of the angle between the star vector and the measured gravity vector, and the gravity vector is assumed to be along negative $\mathbf{r}$, then the measurements become

$$m_i = -\cos\alpha_i$$

The dot product of the unit gravity vector (as a function of ϕ and λ) with the known unit star vector yields the two equations

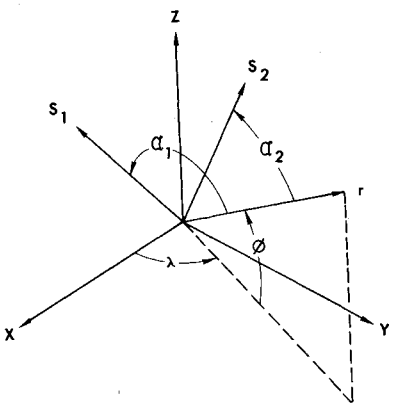

Fig. 1 Position determination with two star-gravity measurements.

Presented as Paper 71-900 at the AIAA Guidance, Control and Flight Mechanics Conference, Hempstead, N.Y., August 16–18, 1971; submitted August 19, 1971; revision received December 27, 1971.

Index category: Spacecraft Navigation, Guidance, and Flight Path Control Systems.

* Staff Engineer, Systems Analysis and Software Department, TRW Houston Operations.

† Member of Technical Staff, Systems Analysis and Software Department, TRW Houston Operations.

‡ Aerospace Technologist, Mission Planning and Analysis Division.

$$-m_i = \cos\phi\cos\lambda S_{i1} + \cos\phi\sin\lambda S_{i2} + \sin\phi S_{i3} \quad (i = 1, 2)$$

where

$$\mathbf{S}_i^T = (S_{i1}, S_{i2}, S_{i3})$$

These two equations can be solved for ϕ and λ. In the simple case where

$$\mathbf{S}_1^T = (0, 1, 0)$$
$$\mathbf{S}_2^T = (0, 0, 1)$$

the ϕ and λ are given by

$$\phi = 90 - \alpha_2$$
$$\lambda = -\sin^{-1}(m_1/\cos\phi)$$

The least squares method for processing measurements is developed by first defining a derived measurement at a known time, t_i, to be

$$m_i = \mathbf{S}_{mi}^T \mathbf{U}_{gmi} \tag{1}$$

where $\mathbf{S}_{mi}$, $\mathbf{U}_{gmi}$ are the measured unit star vector and measured unit gravity vector in a common coordinate system (measurements are assumed to be obtained at the same time, or else that no rotation of the coordinate system occurs between the two measurements). m_i is the derived measurement and represents the cosine of the angle between the star vector and the gravity vector.

Next, a computed measurement is obtained from the catalogued unit star vector, an estimate of the vehicle position, and the gravitational potential of the planet by

$$\hat{m}_i = \mathbf{S}_i^T B_i \mathbf{U}_g(\hat{\phi}, \hat{\lambda}) \tag{2}$$

where $\mathbf{S}_i$ is the catalogued unit star vector (the star vector can be adjusted for the aberration effect of the planet surface velocity relative to the sun). B_i is the transformation from the planet fixed coordinate system to the coordinate system used for the star vectors at the time of the ith star measurement. $\hat{\phi}, \hat{\lambda}$ are the estimated latitude and longitude of the vehicle. $\mathbf{U}_g(\hat{\phi}, \hat{\lambda})$ is the computed unit gravity vector. $\hat{m}_i$ is the computed measurement.

Finally, an iterative least-squares estimate for ϕ and λ is written

$$\begin{bmatrix}\hat{\phi}\\ \hat{\lambda}\end{bmatrix}_{i+1} = \begin{bmatrix}\hat{\phi}\\ \hat{\lambda}\end{bmatrix}_i + \left[\sum_j \frac{1}{\sigma_j^2}\mathbf{A}_j\mathbf{A}_j^T\right]^{-1} \sum_j \frac{\mathbf{A}_j}{\sigma_j^2}[m_j - \hat{m}_j(\hat{\phi}_i, \hat{\lambda}_i)] \tag{3}$$

where

$$\sigma_j^2 = \sigma^2(1 - \hat{m}_j^2)$$

σ^2 is the sum of the variances for angular measurement errors of the star vector and the gravity vector.

$$\mathbf{A}_j^T = \mathbf{S}_j^T B_j[\partial \mathbf{U}_g/\partial(\phi, \lambda)]$$

is the partial derivative vector of the measurement with respect to ϕ and λ. The term $(1 - \hat{m}_j^2)$ results from assuming an angular measurement error while processing the cosine of the angle as the measurement.

For most applications, the partial of the gravity vector can be determined by using only the inverse square portion of the gravity vector. Thus,

$$\mathbf{U}_g \triangleq -\mathbf{U}_r = -\begin{bmatrix}\cos\phi\cos\lambda\\ \cos\phi\sin\lambda\\ \sin\phi\end{bmatrix}$$

$$\frac{\partial \mathbf{U}_g}{\partial(\phi, \lambda)} = \begin{bmatrix}\cos\lambda\sin\phi & \sin\lambda\cos\phi\\ \sin\lambda\sin\phi & -\cos\phi\cos\lambda\\ -\cos\phi & 0\end{bmatrix}$$

or

$$\frac{\partial \mathbf{U}_g}{\partial(\phi, \lambda)} = [\mathbf{U}_1, \mathbf{U}_2\cos\phi] \tag{4}$$

where $\mathbf{U}_1$, $\mathbf{U}_2$, and $\mathbf{U}_r$ are orthonormal vectors and $\mathbf{U}_r$ is the unit position vector in the planet fixed system.

From the equations for $\mathbf{A}_j$ and σ_j, it can be seen that an indeterminate form will occur when the star vector is along the radius vector. Therefore, special procedures must be used for star vectors nearly colinear with the radius vector. These procedures are not considered in the remainder of this paper because they are not required for the Apollo missions.

Gravity Model Errors

An error in the gravity function $\Delta\mathbf{g}$ results in an error in the unit gravity vector of

$$\begin{aligned}\Delta\mathbf{U}_g &= (I - \mathbf{U}_g\mathbf{U}_g^T)\Delta\mathbf{g}/g, \quad \text{or approximately}\\ &= (\mathrm{I} - \mathbf{U}_r\mathbf{U}_r^T)\Delta\mathbf{g}/\mathrm{g}\end{aligned} \tag{5}$$

where I is the identity matrix and g is the gravity acceleration magnitude.

Because $\mathbf{U}_r$ is in the null space of $I - \mathbf{U}_r\mathbf{U}_r^T$, the component of $\Delta\mathbf{g}$ along $\mathbf{U}_r$ does not contribute to $\Delta\mathbf{U}_g$. Thus the error in the unit gravity vector can be written:

$$\Delta\mathbf{U}_g = [\mathbf{U}_1, \mathbf{U}_2, 0]\Delta\mathbf{g}/g$$

or

$$\Delta\mathbf{U}_g = [\mathbf{U}_1, \mathbf{U}_2\cos\phi]\begin{bmatrix}\Delta g_1\\ \Delta g_2/\cos\phi\end{bmatrix}\Big/ g \tag{6}$$

where Δg_1, Δg_2 are the components of the gravity vector errors along the previously defined vectors $\mathbf{U}_1$ and $\mathbf{U}_2$ when these vectors are expressed in the coordinate system used to measure the gravity vector.

The effect of the unit gravity vector error on the solution for ϕ and λ is given by

$$\Delta\begin{bmatrix}\phi\\ \lambda\end{bmatrix} = -\left[\sum_j \frac{1}{\sigma_j^2}\mathbf{A}_j\mathbf{A}_j^T\right]^{-1} \sum_j \frac{1}{\sigma_j^2}\mathbf{A}_j\mathbf{S}_j^T B_j \Delta\mathbf{U}_g \tag{7}$$

By using the relationship

$$\mathbf{S}_j^T B_j \Delta\mathbf{U}_g = \mathbf{A}_j^T\begin{bmatrix}\Delta g_1\\ \Delta g_2/\cos\phi\end{bmatrix}\Big/ g$$

the error in ϕ and λ reduces to

$$\Delta\begin{bmatrix}\phi\\ \lambda\end{bmatrix} = -\begin{bmatrix}\Delta g_1\\ \Delta g_2/\cos\phi\end{bmatrix}\Big/ g \tag{8}$$

The error in the unit gravity vector directly affects the solution for ϕ and λ (with the expected scaling in λ by $\sec\phi$). Because this error is not affected by the number of measurements, it determines the limiting accuracy of the filter.

Numerical Results

The convergence properties of this filter are illustrated in Fig. 2 where the solutions for six iterations based upon four star measurements are plotted. A central force field was used to define the measured gravity vector, and then a central force field and a NASA L1 model with coefficients scaled by 1000 were used in the filter to process the data. A converged solution was obtained after four iterations with initial position errors of 30° in both

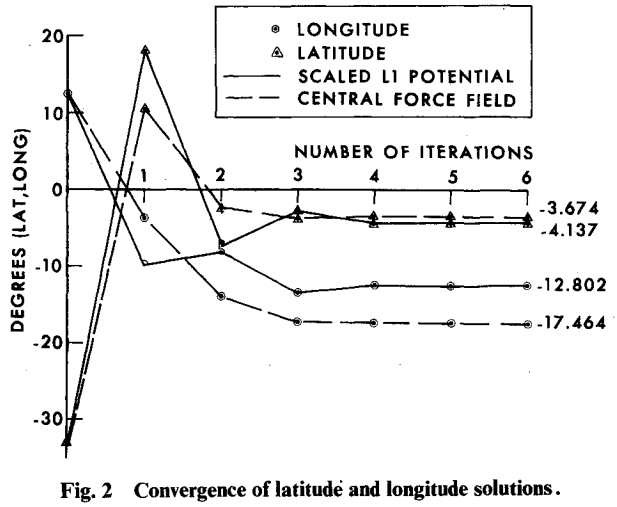

Fig. 2 Convergence of latitude and longitude solutions.

Table 1 Apollo landing site solutions

Apollo mission		Latitude, degs[a]	Latitude solution sigma, degs	Longitude, degs	Longitude solution sigma, degs
Apollo 11	Star/g	0.612	0.020	23.498	0.014
	Best	0.647	0.020	23.505	0.006
Apollo 12	Star/g	−3.045	0.025	−23.423	0.018
	Best	−3.043	0.014	−23.416	0.004
Apollo 14	Star/g	−3.652	0.021	−17.466	0.018
	Best	−3.650	0.014	−17.478	0.004

[a] 0.001° is approximately 100 ft on lunar surface.

ϕ and λ. The effect of the erroneous potential model is evident in the characteristics of the convergence and in the final solution. The error in the final solution is 0.463° in ϕ and 4.662° in λ, which agrees within 5% with that obtained using Eq. (8).

The filter defined herein has been used on the Apollo program for missions 11, 12, and 14 to determine the landing coordinates of the Lunar Module. The solutions obtained from the star-gravity filter and the solutions currently considered to be the best landing site estimates are given in Table 1.

The noise used for processing these mission data was 1.0 mrad and is reflected in the solution standard deviation. However, the solution accuracy does not include gravity model uncertainties (the L1 potential model was used for processing these mission data). The best solutions given for comparison were those obtained from all solution sources, including the following: a) Command Module optical tracking of Lunar Module, b) Lunar Module radar tracking of Command Module, and c) Lunar mapping verified by visual sightings.

The solution accuracy given for the best solution was estimated from the manned spaceflight tracking accuracy, the accuracy of the Command Module sextant and the Lunar Module radar, and the accuracy of lunar maps. The comparison of these results indicate that the performance of the filter is reasonably close to the predicted performance.

Conclusions

A filter has been developed to determine position on a planet surface from measurements of star vectors and gravity vectors in a common coordinate system. An advantage in this formulation is the allowance of a measurement coordinate frame which changes between sets of star-gravity measurements. The accuracy of this filter has been shown to be comparable to other available solutions for the Apollo landing missions and to have a limiting accuracy determined by the uncertainty of the potential model. In summary, this technique appears to provide a viable method for determining position on a planet surface.

Cone Transitional Boundary-Layer Structure at $M_e = 14$

MICHAEL C. FISCHER* AND LEONARD M. WEINSTEIN*
NASA Langley Research Center, Hampton, Va.

Nomenclature

M = Mach number
P = pressure, N/m^2
$\dot{q}$ = convective heat-transfer rate, W/m^2
Re/m = local unit Reynolds number
T = temperature, °K
x = distance along cone surface from tip, m
y = distance perpendicular to cone surface, cm
δ = boundary-layer thickness, $dP_{t,2}/dy = 0$, cm
δ^* = displacement thickness, cm
θ = momentum thickness, cm
ϕ_{spread} = disturbance total spreading angle, deg.
ϕ_{wall} = disturbance spreading angle relative to wall, deg.
α = angle of attack, deg.

Subscripts
2 = behind normal shock
e = boundary-layer edge conditions
survey = survey station
t = total conditions
tr = start of transition
w = wall condition
∞ = freestream condition

Received September 28, 1971.

* Aerospace Engineers, Viscous Flows Section, Hypersonic Vehicles Division.

In classical boundary-layer analysis, three general flow regimes may be distinguished dependent on the stability of the flow[1]; steady laminar flow, nonsteady laminar flow oscillations-transitional flow, and turbulent flow. The second regime, that dealing with the growth of the initial instability into developed turbulent flow, is the least understood and most difficult to model. Results from studies using hot-wire and hot-film instrumentation[2-7] indicate that significant oscillations occur far upstream of the transition location at the surface. At low speeds the large oscillations in the laminar boundary layer apparently do not influence the mean laminar velocity profile or the thickness parameters δ, δ^*, and θ, since good agreement with the laminar Blasius solution has been obtained.[2,3] However, at high speeds, more extreme oscillations occur ahead of the surface transition location[4-7]; consequently, the growth of disturbances at the boundary-layer edge may significantly alter the "laminar" boundary-layer profiles, thicknesses, and integral parameters. Morkovin[8] points out that a significantly altered transition region probably occurs at hypersonic speeds as compared to lower speeds.

This Note proposes to determine if the laminar profiles and thicknesses are altered significantly in the outer half of a hypersonic boundary layer upstream of the nominal wall transition location. The tests were conducted in the Mach 20 leg of the Langley High Reynolds Number Helium facility which has a 1.525-m-diam test section and an axisymmetric contoured

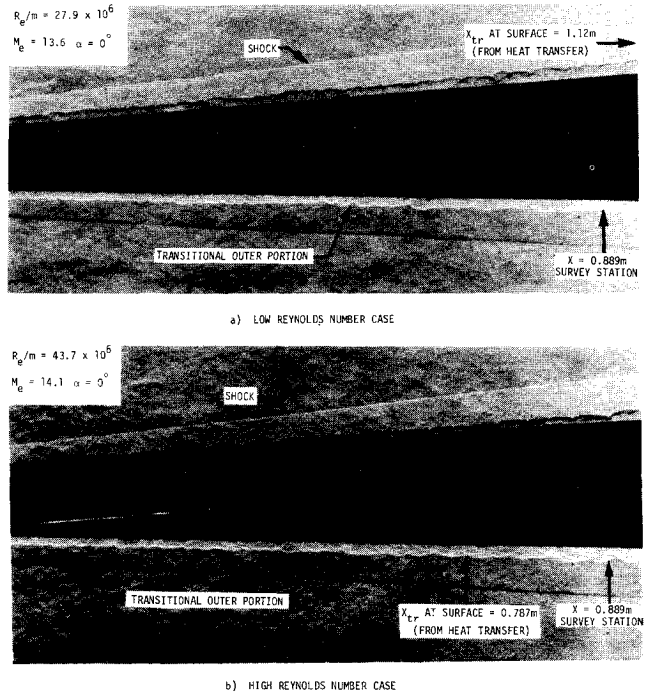

Fig. 1 Spark schlierens of a 2.87° half-angle cone in helium at $M_\infty \approx 18$.